Institute for Shock Physics Internal Report 01-XX

ISOTROPIC MATERIAL MODELS FOR THE ELASTIC RESPONSE OF SAPPHIRE AND QUARTZ SINGLE CRYSTALS UNDER SHOCK WAVE LOADING

J. M. Winey, R. Feng, and Y. M. Gupta

December, 2001

I. INTRODUCTION

This report describes material models for the elastic response of sapphire (c-axis and a-axis orientations) and α-quartz (z-axis and x-axis orientations). The results presented are intended for use in 1-D wave propagation simulations using wave codes such as COPS. Although we derived these models from reported elastic constants, the models assume that the materials are isotropic. We approximated the anisotropy of the real materials by developing different models for different orientations of the crystal. However, these isotropic models can never capture the true anisotropic nature of the crystals. Therefore, the models must be used with some caution, particularly with regard to the lateral stress response.

II. FINITE STRAIN THEORY FOR ANISOTROPIC ELASTIC RESPONSE

Consider a finite elastic deformation such that a material element with initial coordinates a_i is displaced to a position with final coordinates x_i. The Lagrangian (or Green) strains η_{ij} are then defined as

$$\eta_{ij} = \frac{1}{2}\left[\frac{\partial x_k}{\partial a_i}\frac{\partial x_k}{\partial a_j} - \delta_{ij}\right] \tag{1}$$

where δ_{ij} is the Kronecker delta. In this and following equations, the Einstein summation convention is used. The Cauchy stresses σ_{ij} can now be written as a Taylor series expansion in the Lagrangian strains about the initial configuration a_i:[1]

$$\sigma_{ij} = \frac{\rho}{\rho_0}\frac{\partial x_i}{\partial a_k}\frac{\partial x_j}{\partial a_l}\left[C_{klmn}\eta_{mn} + \frac{1}{2}C_{klmnpq}\eta_{mn}\eta_{pq} + \frac{1}{6}C_{klmnpqst}\eta_{mn}\eta_{pq}\eta_{st} + \cdots\right]. \tag{2}$$

The coefficients C_{ijkl}, C_{ijklmn}, and $C_{ijklmnpq}$ are the second-order, third-order, and fourth-order elastic constants, respectively. Since we are interested in wave propagation, we consider only

the adiabatic elastic constants. The stresses and the strains are defined to be positive in tension. Therefore, the compressive mean stress is defined as

$$\bar{P} = -[\sigma_{11} + \sigma_{22} + \sigma_{33}]/3. \tag{3}$$

Note that the mean stress will in general be different for different loading conditions. For instance, the mean stress for uniaxial strain along a particular crystal orientation will generally be different from the mean stress under hydrostatic compression and from the mean stress for uniaxial strain along a different crystal orientation.

The models we developed decompose the stresses into the mean stress and the stress deviators s_{ij}:

$$\sigma_{ij} = -\bar{P}\delta_{ij} + s_{ij}. \tag{4}$$

We assume that the materials are isotropic and the stress deviators are small compared to the mean stress (a questionable approximation for sapphire and quartz). Under these approximations, the mean stress is equivalent to the thermodynamic pressure (determined using an equation of state) and the elastic response of the material is described by the mean stress (bulk) response and the shear modulus. Models of this type are called *pressure-deviator models*.

A. Uniaxial Compression Along the *z*-Axis

For uniaxial strain along the *z*-axis, the only nonzero strain component is η_{33}. Also, we have

$$\frac{\partial x_1}{\partial a_1} = \frac{\partial x_2}{\partial a_2} = 1; \quad \frac{\partial x_3}{\partial a_3} = \frac{\rho_0}{\rho}. \tag{5}$$

All other $\partial x_i/\partial a_j$ are zero. Therefore, the Cauchy stresses from Eq. 2 (up to third-order in strain) are

$$\sigma_{11} = \frac{\rho}{\rho_0}\left[C_{1133}\eta_{33} + \frac{1}{2}C_{113333}\eta_{33}^2 + \frac{1}{6}C_{11333333}\eta_{33}^3 \right] \tag{6a}$$

$$\sigma_{22} = \frac{\rho}{\rho_0}\left[C_{2233}\eta_{33} + \frac{1}{2}C_{223333}\eta_{33}^2 + \frac{1}{6}C_{22333333}\eta_{33}^3 \right] \tag{6b}$$

$$\sigma_{33} = \frac{\rho_0}{\rho}\left[C_{3333}\eta_{33} + \frac{1}{2}C_{333333}\eta_{33}^2 + \frac{1}{6}C_{33333333}\eta_{33}^3 \right]. \tag{6c}$$

For the case of uniaxial strain, the compression parameter $\mu = \rho/\rho_0 - 1$ is related to the Lagrangian strain by

$$\eta_{33} = -\frac{(2+\mu)\mu}{2(1+\mu)^2}. \tag{7}$$

For z-axis compression, the COPS models are derived from the finite strain results through a process involving several steps:

1) The compressive longitudinal stress, P_z (= $-\sigma_{33}$), is plotted as a function of μ from Eq. 6(c). This curve is fitted using a cubic polynomial, with the coefficient of the first term set equal to C_{3333}.
2) The compressive mean stress, $\bar{P}$, is plotted as a function of μ using Eq. 3 with the stresses from Eqs. 6(a-c). This curve is fitted using a cubic polynomial, with the coefficient of the first term set equal to the bulk modulus. The effective bulk modulus for uniaxial z-axis compression is defined as

$$B_z = (C_{1133} + C_{2233} + C_{3333})/3. \tag{8}$$

3) An effective shear modulus, as a quadratic function of the mean stress, is determined from the difference between the longitudinal and mean stress curves. This procedure treats the material as if it is an isotropic elastic solid.

B. Uniaxial Compression Along the *x*-Axis

For uniaxial strain along the *z*-axis, the only nonzero strain component is η_{11}. Also, we have

$$\frac{\partial x_2}{\partial a_2} = \frac{\partial x_3}{\partial a_3} = 1\,; \quad \frac{\partial x_1}{\partial a_1} = \frac{\rho_0}{\rho}\,. \tag{9}$$

All other $\partial x_i / \partial a_j$ are zero. Therefore, the Cauchy stresses from Eq. 2 (up to third-order in strain) are

$$\sigma_{11} = \frac{\rho_0}{\rho}\left[C_{1111}\eta_{11} + \frac{1}{2}C_{111111}\eta_{11}^2 + \frac{1}{6}C_{11111111}\eta_{11}^3 \right] \tag{10a}$$

$$\sigma_{22} = \frac{\rho}{\rho_0}\left[C_{2211}\eta_{11} + \frac{1}{2}C_{221111}\eta_{11}^2 + \frac{1}{6}C_{22111111}\eta_{11}^3 \right] \tag{10b}$$

$$\sigma_{33} = \frac{\rho}{\rho_0}\left[C_{3311}\eta_{11} + \frac{1}{2}C_{331111}\eta_{11}^2 + \frac{1}{6}C_{33111111}\eta_{11}^3 \right]. \tag{10c}$$

Once again, the compression parameter $\mu = \rho/\rho_0 - 1$ is related to the uniaxial Lagrangian strain by

$$\eta_{11} = -\frac{(2+\mu)\mu}{2(1+\mu)^2}\,. \tag{11}$$

For x-axis compression, the COPS models are derived from the finite strain results in a manner similar to the z-axis case:

1) The compressive longitudinal stress, P_x (= $-\sigma_{11}$), is plotted as a function of μ from Eq. 10(a). This curve is fitted using a cubic polynomial, with the coefficient of the first term set equal to C_{1111}.
2) The compressive mean stress, $\overline{P}$, is plotted as a function of μ using Eq. 3 with the stresses from Eqs. 10(a-c). This curve is fitted using a cubic polynomial, with the coefficient of the first term set equal to the bulk modulus. The effective bulk modulus for uniaxial x-axis compression is defined as

$$B_x = \left(C_{1111} + C_{1122} + C_{1133}\right)/3. \tag{12}$$

3) An effective shear modulus, as a quadratic function of the mean stress, is determined from the difference between the longitudinal and mean stress curves. As with the z-axis case, this procedure treats the material as if it is an isotropic elastic solid.

III. MODELS FOR *c*-AXIS AND *a*-AXIS SAPPHIRE

For c-axis (i.e. z-axis) and a-axis (i.e. x-axis) compression, the relevant second-order[2] and third-order[3] elastic constants of sapphire are:

C_{1111} = 497.6 GPa, C_{1122} = 162.6 GPa, C_{1133} = 117.2 GPa, C_{3333} = 501.8 GPa
C_{111111} = -3870 GPa, C_{111122} = -1090 GPa, C_{111133} = -963 GPa, C_{113333} = -922 GPa, C_{333333} = -3340 GPa

The density of sapphire is 3.985 g/cc (Ref. 4); the Gruneisen parameter is Γ = 1.28 (Refs. 5,6). Using the elastic constants given above, COPS models were developed for c-axis and a-axis shock compression. Since the fourth-order elastic constants for sapphire are not available, the

stresses from Eq. 2 were calculated only to second-order in strain. However, due to the high stiffness of sapphire, no significant error results from this limitation.

For c-axis compression, the procedures of Section II yield the following mean stress curve and effective shear modulus. The units for the mean stress and the effective shear modulus are GPa.

$$\overline{P} = 245.4\mu + 400.4\mu^2 - 1680\mu^3 \tag{13a}$$

$$G = 192.3 + 0.7534\overline{P} - 0.0653\overline{P}^2 \tag{13b}$$

Calculations of longitudinal and mean stress using the c-axis model for sapphire are compared with Hugoniot data and with the results of anisotropic finite strain calculations (from Eq. 6(a-c)) in Fig. 1.

For a-axis compression, the mean stress curve and effective shear modulus are, in units of GPa:

$$\overline{P} = 259.1\mu + 520.3\mu^2 - 2061\mu^3 \tag{14a}$$

$$G = 178.9 + 1.512\overline{P} - 0.0726\overline{P}^2 \tag{14b}$$

Calculations of longitudinal and mean stress using the a-axis model for sapphire are compared with Hugoniot data and with the results of anisotropic finite strain calculations (from Eq. 10(a-c)) in Fig. 2.

These two models for sapphire are in agreement with the elastic constants for longitudinal stresses up to ~20 GPa, which is above the HEL for c-axis (13 - 15 GPa)[4] and a-axis (17 - 19 GPa)[7] compression.

IV. MODELS FOR *z*-AXIS AND *x*-AXIS QUARTZ

For *z*-axis and *x*-axis compression, the relevant second-order[8] and third-order[9] elastic constants of quartz are:

C_{1111} = 86.8 GPa, C_{1122} = 7.04 GPa, C_{1133} = 11.91 GPa, C_{3333} = 105.8 GPa
C_{111111} = -210 GPa, C_{111122} = -345 GPa, C_{111133} = +12.0 GPa, C_{113333} = -312 GPa, C_{333333} = -815 GPa

The fourth-order constants have been measured for the longitudinal response only. The results are:

$C_{11111111}$ = 15,930 GPa,[10] $C_{33333333}$ = 17,480 GPa[11]

The density of quartz is 2.6485 g/cc (Ref. 8); the Gruneisen parameter is $\Gamma = 0.675$ (Ref. 12). Using the elastic constants given above, COPS models were developed for *z*-axis and *x*-axis shock compression. In developing these models, the longitudinal stresses were calculated from Eq. 2 to third-order in strain, using the fourth-order elastic constants. However, the lateral stresses could only be calculated to second-order in strain. Therefore, while the longitudinal response from the models given below is accurate, *the lateral response is only approximate.*

For <u>*z*-axis compression</u>, the procedures of Section II yield the following mean stress curve and effective shear modulus. The units for the mean stress and the effective shear modulus are GPa.

$$\overline{P} = 43.19\mu + 156.2\mu^2 + 48.60\mu^3 \tag{15a}$$

$$G = 46.92 + 1.873\overline{P} + 0.3459\overline{P}^2 \tag{15b}$$

Calculations of longitudinal and mean stress using the *z*-axis model for quartz are compared with Hugoniot data and with the results of anisotropic finite strain calculations (from Eq. 6(a-c)) in Fig. 3.

For *x*-axis compression, the mean stress curve and effective shear modulus are, in units of GPa:

$$\bar{P} = 35.25\mu + 31.57\mu^2 + 270.7\mu^3 \tag{16a}$$

$$G = 38.66 - 2.358\bar{P} + 1.093\bar{P}^2 \tag{16b}$$

Calculations of longitudinal and mean stress using the *x*-axis model for quartz are compared with Hugoniot data and with the results of anisotropic finite strain calculations (from Eq. 10(a-c)) in Fig. 4.

These models for quartz are in agreement with the elastic constants for longitudinal stresses up to ~10 GPa., which is well above the HEL for *z*-axis (~6 GPa)[11] and *x*-axis (~5 GPa)[13] compression.

REFERENCES

1. For a more detailed development, see M. P. Conner, Masters Thesis, Washington State Univeristy, 1988, Chapter Two.
2. J. H. Gieske and G. R. Barsch, *Phys. Stat. Sol.* **29**, 121 (1968)
3. R. E. Hankey and D. E. Schuele, *J. Acoust. Soc. Am.* **48**, 190 (1970)
4. L. M. Barker and R. E. Hollenbach, *J. Appl. Phys.* **41**, 4208 (1970)
5. J. H. Gieske, Ph.D. Dissertation, Pennsylvania State Univeristy, 1968
6. B. Yates, R. F. Cooper, A. F. Pojur, *J. Phys. C: Solid State Phys.* **5**, 1046 (1972)
7. S. C. Jones, B. A. M. Vaughen, and Y. M. Gupta, unpublished
8. H. J. McSkimin, P. Andreatch, Jr., and R. N. Thurston, *J. Appl. Phys.* **36**, 1624 (1965)
9. R. N. Thurston, H. J. McSkimin, and P. Andreatch, Jr., *J. Appl. Phys.* **37**, 267 (1966)
10. R. Fowles, *J. Geophys. Res.* **72**, 5729 (1967)
11. S. C. Jones and Y. M. Gupta, *J. Appl. Phys.* **88**, 5671 (2000)
12. R. Boehler, A. Skoropanov, D O'Mara, and G. C. Kennedy, *J. Geophys. Res.* **84**, 3527 (1979)
13. R. A. Graham, F. W. Neilson, and W. B. Benedick, *J. Appl. Phys.* **36**, 1775 (1965)

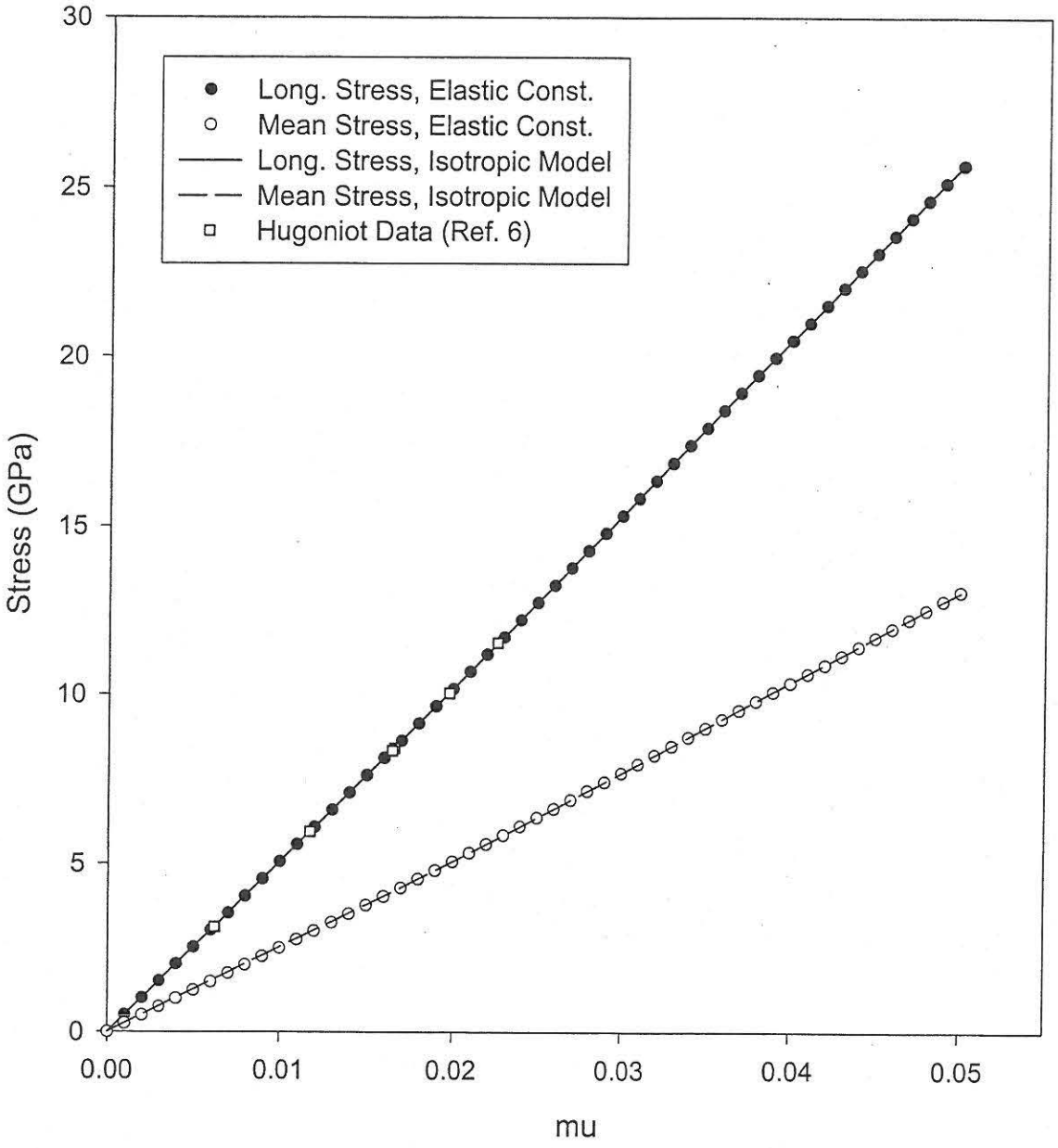

Figure 1 – Stress versus compression for *c*-axis sapphire. The circles represent the results of calculations (from Eqs. 6(a-c)) using the elastic constants of sapphire. The lines result from calculations using the isotropic model from Eqs. 13(a-b). The open squares are the Visar data from Ref. 4.

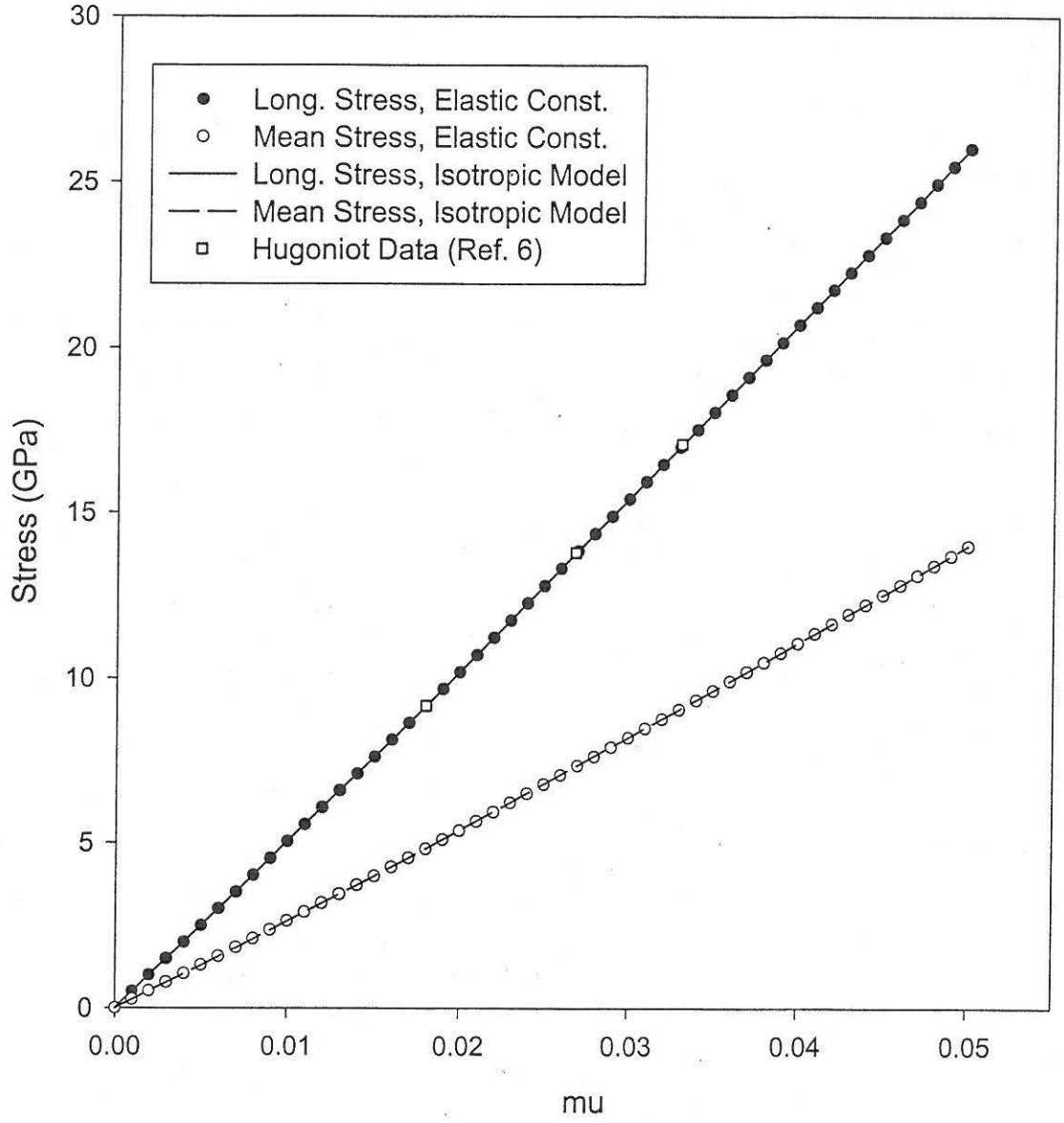

Figure 2 – Stress versus compression for *a*-axis sapphire. The circles represent the results of calculations (from Eqs. 10(a-c)) using the elastic constants of sapphire. The lines result from calculations using the isotropic model from Eqs. 14(a-b). The open squares are the Visar data from Ref. 7.

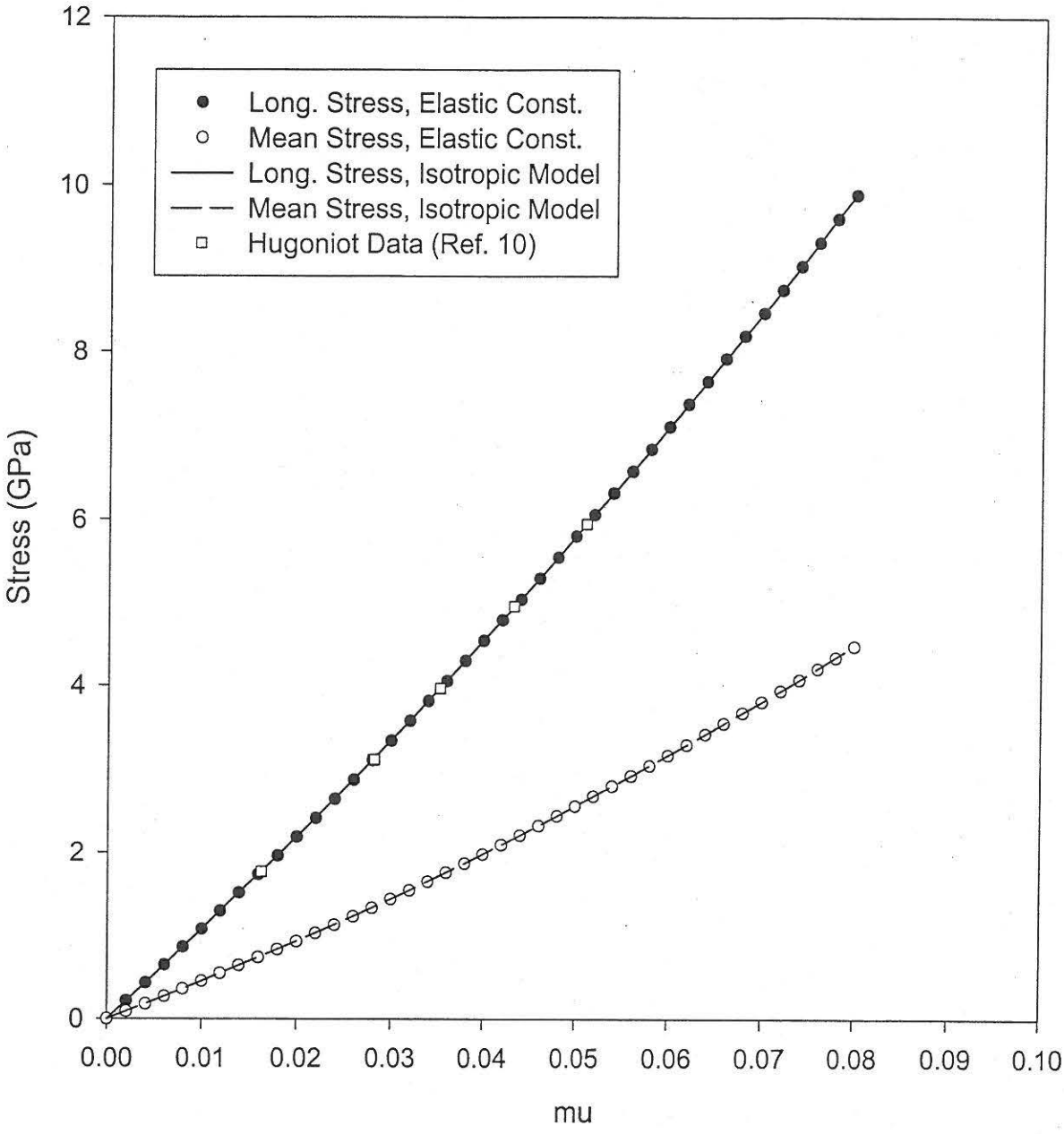

Figure 3 – Stress versus compression for *z*-axis quartz. The circles represent the results of calculations (from Eqs. 6(a-c)) using the elastic constants of quartz. The lines result from calculations using the isotropic model from Eqs. 15(a-b). The open squares are the Visar data from Ref. 11.

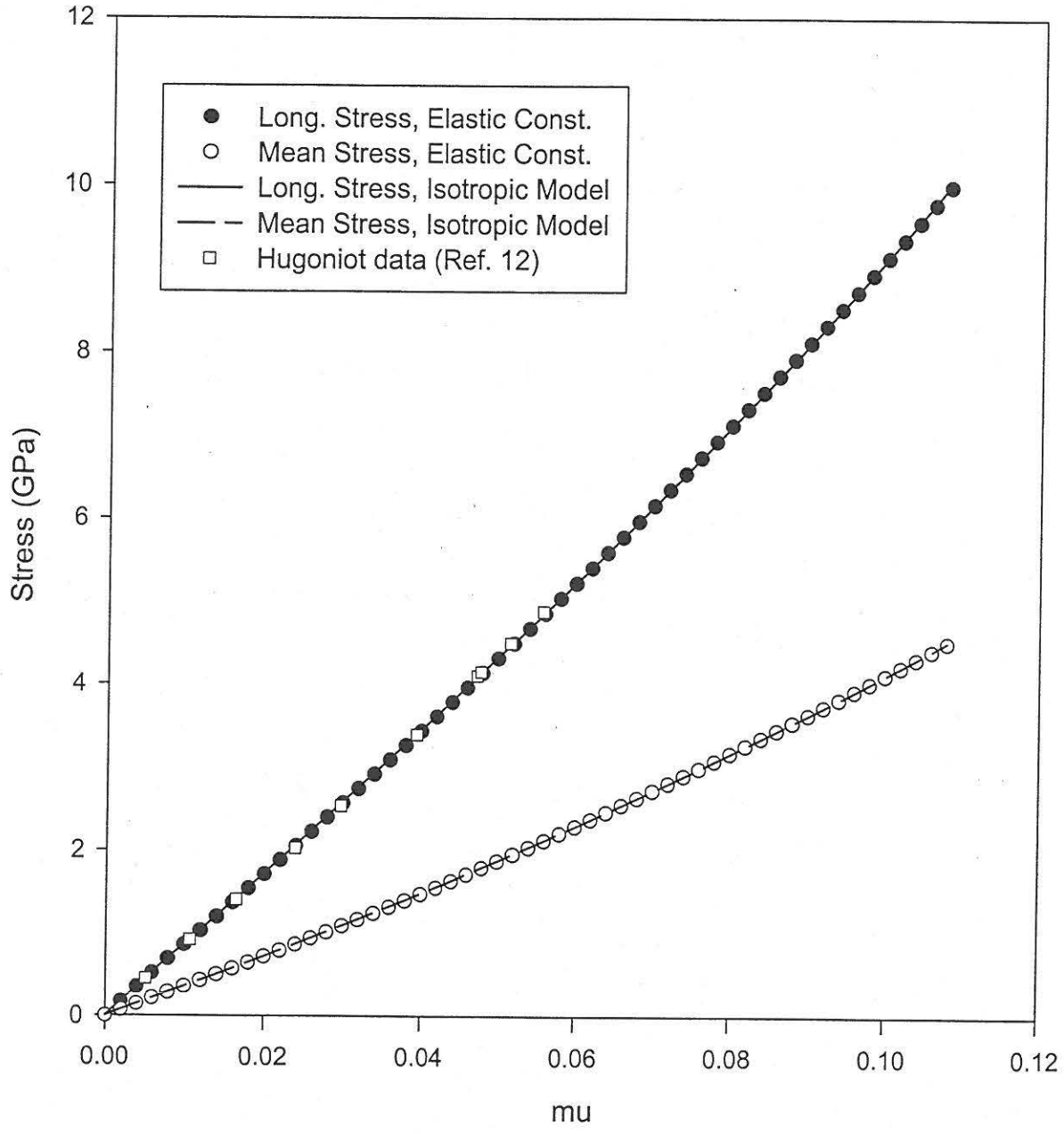

Figure 4 – Stress versus compression for *x*-axis quartz. The circles represent the results of calculations (from Eqs. 10(a-c)) using the elastic constants of quartz. The lines result from calculations using the isotropic model from Eqs. 16(a-b). The open squares are the Hugoniot data from Ref. 13.